

Development and Control of a Roadway Seam Tracking Mobile Robot

Hyun Taek Cho*, Poongwoo Jeon**, and Seul Jung***

Intelligent Systems and Emotional Engineering Lab.

Department of Mechatronics Engineering

Chungnam National University, Daejeon, Korea

(+82-42-821-6876, *hyuntaek@kebi.com, **windrainer@hanmail.net, ***jungs@cnu.ac.kr)

Abstract: In this paper, a crack sealing robot is developed. The crack sealing robot is built to detect, track, and seal the crack on the pavement. The sealing robot is required to brush all dirt in the crack out for preparing a better sealing job. Camera calibration has been done to get accurate crack position. In order to perform a cleaning job, the explicit force control method is used to regulate a specified desired force in order to maintain constant contact with the ground. Experimental studies of force tracking control are conducted under unknown environment stiffness and location. Crack tracking control is performed. Force tracking results are excellent and the robot finds and tracks the crack very well.

Keywords: Crack sealing robot, Crack detection, Explicit force control, laser sensor

1. INTRODUCTION

Researches on automated highway have been conducting in various ways : autonomous car platoon, autonomous traffic flow control, and autonomous highway maintenance. Researches on autonomous car platoon and autonomous traffic flow control have mainly been done at the center of PATH located UC Berkeley, in USA. On the other hand, researches on autonomous maintenance have been mainly conducted by the center of AHMCT at UC Davis supported by CALTRAN. The advanced highway maintenance and construction technology (AHMCT) center at UC Davis is one of the leading group in the world for autonomous maintenance. The main goal of autonomous maintenance and construction technology is to automate working environment on the road way because works at the road are very dangerous for workers due to fast passing cars.

Cracks on the highway may cause uncomfortable driving condition to the driver, even the traffic accident by losing control of the car. Preventing these situations, cracks should be sealed by workers. A crack sealing robot is one of their projects [1]. The purpose of the crack sealing robot is to seal cracks on the pavement autonomously. Recently, they have built an autonomous crack sealing automobile that seals cracks on the highway by following almost straight line of cracks [1] that appear at the boundary of two separate paving jobs by the paver.

However, in Korea, the situation is much worse so that high way accidents of workers are increasing every year. So our goal is to conduct feasible research on autonomous maintenance of road way to save labors and lives from the present danger.

In this paper, we have built an autonomous crack sealing mobile robot that finds the crack and follows the crack. Even though the ultimate goal of the sealing robot is to seal the crack



Fig.1 The crack sealing robot working environment.

, as apriori research, the robot has to perform a cleaning job before sealing. The sealing robot is composed of three parts : crack detection, crack sealing, and controllers. The crack detection part finds cracks by laser and camera sensor, sends the position of the crack to the controller. Then the controller actuates two wheels to move the sealing robot to the position where cracks are located in the middle of the robot so that the sealing job is performed easily. The sealing part has 3 degrees of freedom to move x, y, and z direction. The sealing job is done by the gantry robot. In order to perform a better sealing job, the gantry robot has to clean the inside of the crack by brushing all dirt out.

Here, in order to perform brushing task before sealing, force control with the ground is used to maintain constant contact. The crack sealing robot finds crack by using a laser sensor and a vision sensor, and tracks the crack on the pavement while contact force on the ground is regulated. Force control is known as a sophisticated control method that has to control the force as well as the position of the robot.

There have been proposed many force control algorithms. The hybrid force control and impedance force control methods are two main streams[2,3]. Based on these two control

strategies, various modified force control algorithms are proposed [4-11].

In this paper, the performance of the explicit force control algorithm is presented. In our case, the explicit force control is appropriate since it is very simple to regulate desired force directly. It does not require any information about environment location and stiffness even though it has lack of dynamic compensation. Experimental studies of the explicit force control and crack tracking control are conducted.

2. OVERALL SYSTEM STRUCTURE

The developed overall crack sealing robot structure is shown in figure 1. The robot is a mobile manipulator that is a wheeled drive robot with a gantry typed robot in the middle. The robot is actuated by two rear wheels. The robot can make turns by differing the speed of two wheels. The robot is somewhat heavy that control of dynamics of inertia and centrifugal force is not easy for fast movement.

The robot consists of three parts: crack detecting part, crack sealing part, and actuator part. The crack detecting part shown in figure 2 as a black box has a laser sensor and a camera sensor to detect cracks.



Fig. 2 The developed crack sealing robot

Abrupt step change of the crack in sensed information by a laser sensor is obtained by the camera. The crack sealing part has a gantry typed robot that moves xyz directions. X and y direction movements are actuated by timing belts with a LM guide. Z axis movement is actuated by ball screw driven by a DC motor in order to prevent it from falling by gravity force. The force sensor is attached to the z axis so that the normal force to the ground is regulated. The brushing device will also be equipped at the end of z axis in the future. The actuation part shown in figure 1 is located at the rear of the robot and it has batteries, computers, actuating motors, and other necessary hardware.

All actuation is done by DC motors equipped with encoders. Total 5 DC motors are used in the sealing robot. Two for wheels and 3 for the gantry robot are used. Figure 3 shows the control block diagram of the sealing robot. In order to access the JR3 force sensor ISA bus type is required. The dSpace DSP system controls two wheels as well as the gantry type robot.

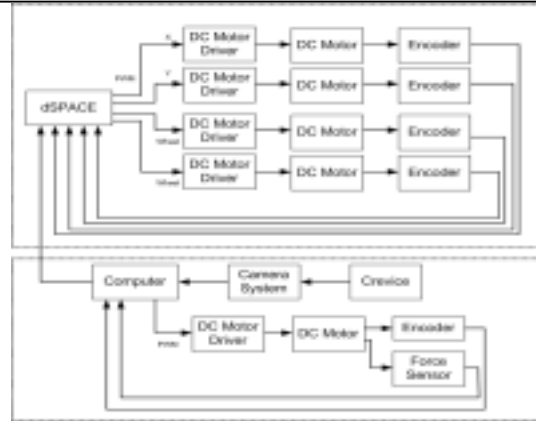


Fig.3 Overall control block

3. CRACK DETECTION

3.1 Crack Detection Setup

Cracks are detected by a laser sensor and a camera sensor. Figure 4 shows the crack detecting system. Crack detecting system in the black box consists of a laser sensor, a camera sensor, and signal processor. A laser sensor generates a constant laser beam on the ground. Since the lightness of the beam is almost consistent reflection is minimized. If any hollow crack is present in the path, the laser beam becomes discontinuous. A camera captures the image of the laser beam and then processes the image to get the crack position. In order for the robot to be aligned with the crack the error is formed as the distance from the location of the laser sensor to the location of the crack as shown in figure 4. The robot actually tries to track the crack by locating it in the middle of the face of the robot. This way simplifies the following cleaning and sealing jobs performed by the gantry robot.

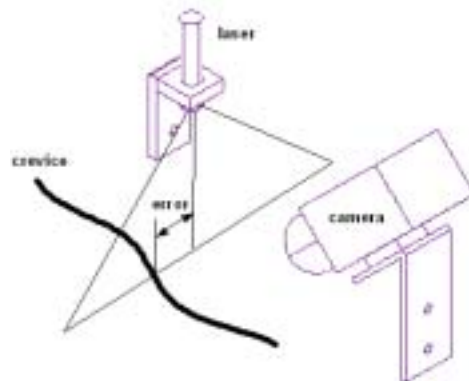


Fig. 4 Crack detection by laser and camera

Real experimental setup of crack detecting is shown in figure 5. The laser sensor is mounted on the middle of the frame of the gantry robot. The camera is located at the middle of the robot head. Since the camera is tilted and located with a certain distance from the laser sensor the captured image may be reflected a little at the boundary due to different focal distances. This should be calibrated before capturing the image. Calibration is done as follows.



Fig.5 Crack detection device setup

3.2 Camera Calibration

The coordinate of camera and laser sensor is shown in figure 6. A point $P(X, Y)$ in the world frame should be appeared as $\bar{p}(\bar{x}, \bar{y})$ in CCD camera frame. But, due to the reflection of camera lens, it appears as $p(x, y)$ and stored as $p(u, v)$ [6-12].

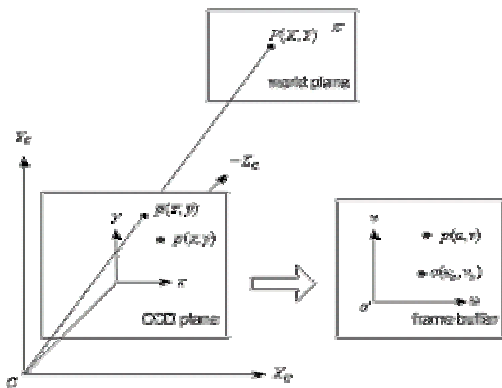


Fig. 6 Camera Coordinates

Considering the radial, decentering, and thin prism reflection yields

$$x = (u - u_0)d_x, y = (v - v_0)d_y \quad (1)$$

$$\bar{x} = x + \delta^{(x)}(x, y), \bar{y} = y + \delta^{(y)}(x, y) \quad (2)$$

where $\delta^{(x)}(x, y)$ and $\delta^{(y)}(x, y)$ are correction function for reflection. Two correction functions are defined as

$$\delta^{(x)}(x, y) = k_1x(x^2 + y^2) + (2p_1xy + p_2(y^2 + 3x^2)) + s_2(x^2 + y^2) \quad (3)$$

$$\delta^{(y)}(x, y) = k_1y(x^2 + y^2) + (2p_1xy + p_2(x^2 + 3y^2)) + s_2(x^2 + y^2) \quad (4)$$

where k_1, p_1, p_2, s_1, s_2 are constants. The world coordinate (X, Y) can be represented by the following equations

$$X = \frac{\sum_{0 \leq i+j \leq 3} a_{ij}^{(1)} u^i v^j}{\sum_{0 \leq i+j \leq 3} a_{ij}^{(3)} u^i v^j}, Y = \frac{\sum_{0 \leq i+j \leq 3} a_{ij}^{(2)} u^i v^j}{\sum_{0 \leq i+j \leq 3} a_{ij}^{(3)} u^i v^j} \quad (4)$$

where $a_{ij}^{(k)}$ is a transformation variable.

The following equation is formed.

$$\rho x_w = A \hat{u} \quad (5)$$

where $\rho = a^{(i)} \hat{u}$ and $x_w = (X, Y, 1)^T$.

$$A = \begin{Bmatrix} a_{33}^{(1)} & \cdots & a_{00}^{(1)} \\ a_{33}^{(2)} & \cdots & a_{00}^{(2)} \\ a_3^{(3)} & \cdots & a_{00}^{(3)} \end{Bmatrix} \quad (6)$$

and

$$\hat{u} = (u^3, u^2v, uv^2, v^3, u^2, uv, v^2, u, v, 1)^T \quad (7)$$

In order to find the transformation matrix, we use neural network to train based on image data. Figure 7 shows the neural network structure.

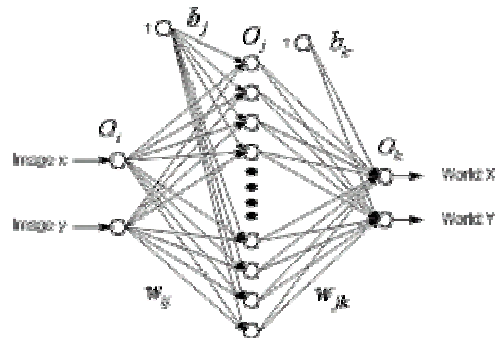


Fig. 7 Neural network structure

In order to calibrate the camera system, image exemplars shown in figure 8 are used as training data.

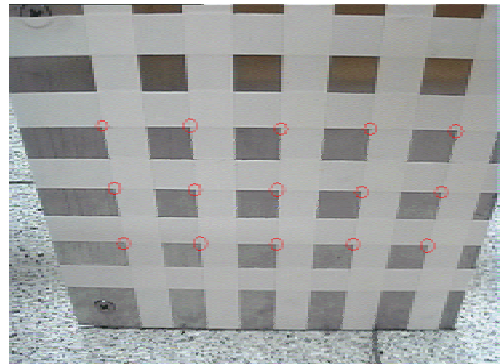


Fig. 8 15 points for image exemplars

Table 1 shows the coordinates of each point.

Table 1 Coordinates of real and image of points

X (m)	-0.0075	-0.035	0.005	0.045	0.085	-0.0075	-0.035	0.005
Y (m)	-0.14	-0.14	-0.14	-0.14	-0.14	-0.18	-0.18	-0.18
X	122	236	353	469	583	136	243	350
Y	163	163	163	165	167	245	246	247
X (m)	0.045	0.085	-0.0075	-0.035	0.005	0.045	0.085	
Y (m)	-0.18	-0.18	-0.22	-0.22	-0.22	-0.22	-0.22	
X	458	563	150	249	348	448	545	
Y	248	249	315	317	319	319	319	

Table 2 shows the points calculated by equation (5) and points generated by NN after training. We can compare two data with real coordinate values. We see that points after neural network training are more accurate.

Table 2 coordinates after NN network learning

X(m)	-0.0075	-0.035	0.005	0.045	0.085
Y(m)	-0.10	-0.10	-0.10	-0.10	-0.10
(5) X(m)	-0.002653830	0.008298339	0.002205258	0.034492940	0.073799017
(5) Y(m)	0.043185350	-0.02308127	-0.06652324	-0.08538817	-0.09243907
NN X(m)	-0.005663	-0.033802	0.006692	0.046648	0.084948
NN Y(m)	-0.111773	-0.112072	-0.112501	-0.111096	-0.110850
X(m)	-0.0075	-0.035	0.005	0.045	0.085
Y(m)	-0.26	-0.26	-0.26	-0.26	-0.26
(5) X(m)	0.002643729	-0.01702806	0.002032269	-0.041240096	0.117923896
(5) Y(m)	-0.02627943	-0.14460892	-0.12377904	0.001108507	-0.34628243
NN X(m)	-0.008088	-0.035905	0.003955	0.044499	0.084552
NN Y(m)	-0.250905	-0.249976	-0.249644	-0.250084	-0.250742

After calibrating camera we take the image of a laser beam. Figure 9 shows the camera captured real image of figure 5. The crack on the floor is detected by the laser sensor. In this case, the crack is located in the middle so that the error is almost zero. Then the robot follows the crack by moving straight ahead.



Fig 9. Image of detected crack position

4. EXPLICIT FORCE CONTROL

In our sealing robot, only z axis requires force control. Our requirement is to make contact with the ground while

regulating certain force. Among many force control algorithms, the explicit force control method is one good candidate since the explicit force control method regulates force errors not position errors. So this is kind of hybrid force control method that separates force controlled direction and position controlled direction completely.

The control law of the explicit force control is formed with force errors. Force error is directly minimized by forming the PID control law. The idea is quite similar to the hybrid force control method in that desired force is regulated directly. It is very convenient that the exact location of the environment is not required since the control law is formed with force errors. On the contrary, this becomes a disadvantage that a larger overshoot of force can be observed at the transition from free space to contact space.

Here, since we are controlling only z axis for force control, compensation for the dynamic of robot is not considered. Since z axis is driven by ball screw, it is more like a linear system. So the force control law of the explicit force control method actually drives the robot.

The explicit force control can be formed as PID controller.

$$\tau = k_p e + k_D \dot{e} + k_I \int e dt \quad (8)$$

where $e = f_d - f_e$ and f_d is the desired force, f_e is the real force from the force sensor. k_p, k_D, k_I are controller gains, and τ is the driving torque.

The robot is driven to minimize the force error. Figure 10 shows the control block diagram of the explicit force control.

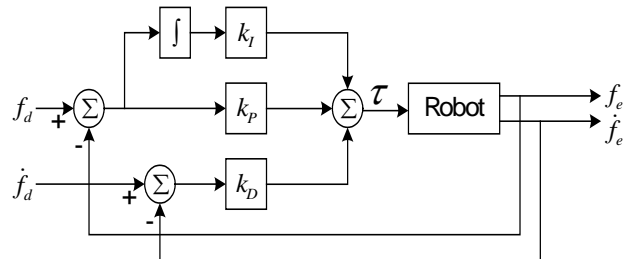


Fig. 10 Explicit force control block

5. MOBILE ROBOT TRACKING CONTROL

The sealing robot is a wheeled driven mobile robot. Figure 11 shows the coordinate of the robot and the crack.

The robot tracks the crack by actuating right and left wheels to make the location of the crack be in the middle of the robot head. So the control algorithm is to minimize the error angle defined in figure 11.

$$\phi_e = \tan^{-1}\left(\frac{S_e}{l}\right) \quad (9)$$

where ϕ_e is the angle error between the crack defined in figure 4 and the center of the wheel axis, S_e is the distance error defined in figure 4, and l is the length from the wheel axis to the robot head as shown in figure 11.

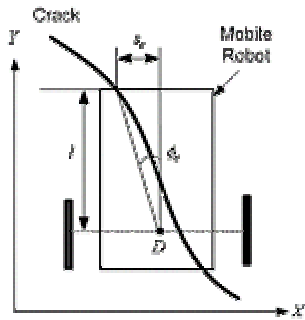


Fig. 11 Crack and robot coordinates

The control command uses a simple PD control for driving right and left wheels. The control laws are

$$w_R^{PWM} = v + p_{gain} \times \phi_e + d_{gain} \times \dot{\phi}_e \quad (10)$$

$$w_L^{PWM} = v - p_{gain} \times \phi_e - d_{gain} \times \dot{\phi}_e \quad (11)$$

where v is the forward velocity of the robot. If there is no error then the robot move forward. The control block diagram of the sealing robot is shown in figure 12.

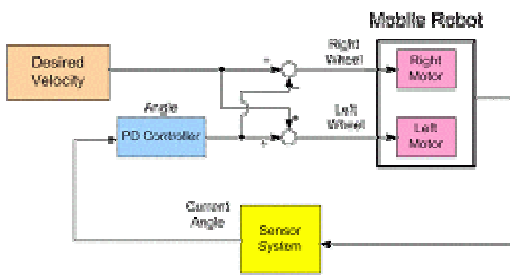


Fig. 12 Control block diagram

6. EXPERIMENTS

6.1 FORCE TRACKING EXPERIMENT

Force control experimental setup is shown in figure 13. Environment is the tile floor and wooden plates. The sealing robot is required to move on the wood, and the floor, then the wood. There is abrupt step change between two wood plates. We do not have any information on the wood and the floor, namely environment location and stiffness are unknown to the robot. The robot is required to track the environment with regulating 10N force. JR3 force sensor is mounted at the end of z axis to detect force and rollers are attached to the end-effector to minimize friction force. Only normal force to the ground is regulated.



Fig. 13 Force control experimental setup

Force tracking result is shown in figure 14. The 10N desired force is well regulated by the explicit force control algorithm. Initially, the robot made contact and followed on the wood while regulating desired force. We observe that losing contact happens at 18 seconds when the robot steps down from the wood to the floor, but the robot immediately made contact and regulated desired force. We also observe the force overshoot when the robot steps up from the floor to the wood plate. Soon the robot regulates desired force very well. From this experiment, we can see the robustness of the explicit force control algorithm under the situation that environment is totally unknown to the robot.

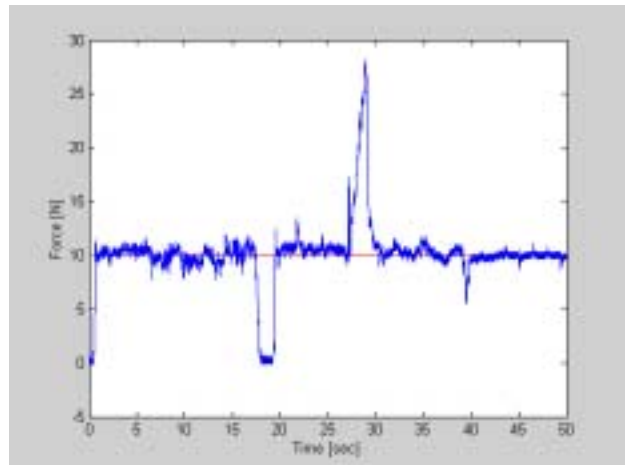


Fig. 15 Explicit PID force control for wood and steel

6.2 CRACK TRACKING EXPERIMENT

Next experiment is for the sealing robot to find and track the crack. The experimental setup of the crack tracking is shown in figure 16. The crack is arbitrary made by two wood plates on the floor. Two plates are located apart so that the crack between two plates can be artificially made. Initially the mobile robot is not aligned with the crack direction. In order to see the robot track the crack. The robot is required to follow the crack in the middle of two wheels. The robot tracks the crack by actuating right and left wheels to make the location of the crack be in the middle of the robot head.



Fig.15 Crack tracking of mobile robot

Figure 13 shows the crack tracking result. Initially the robot starts with error of 8cm, then the robot follows the crack with less than 1cm error. The overshoot observed at around 2 seconds may be caused by dynamic effects of the mobile robot since control is done mainly based on the kinematic modeling. Dynamic effects are wheel slip or other nonlinear dynamic due to the fact that the center of gravity is not aligned with wheel axis. This is the issue of the dynamic model based control of the mobile robot.

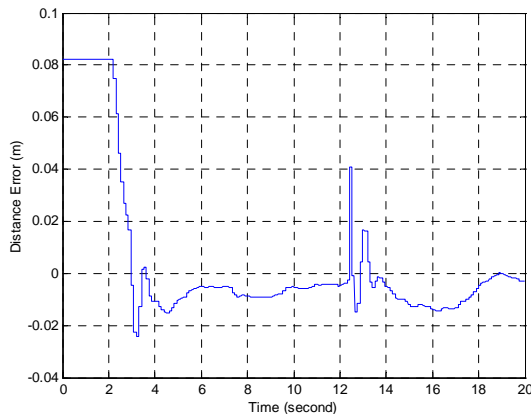


Fig. 16 Crack tracking result

7. CONCLUSIONS

This paper presented the feasibility studies of the crack sealing robot. Experimental studies of crack tracking for the crack sealing robot are conducted. The crack sealing robot is developed to find the crack and track the crack on the pavement while contact force on the ground is regulated. Performances by explicit PID force control are excellent under unknown environment. Crack tracking of the sealing robot was performed by a simple PD controller based on kinematic model. Without considering slip conditions and other nonlinear effects, notable tracking errors due to the dynamic behavior are

observed. Dynamic model based control may be considered to minimize the tracking error.

Our robot is not equipped with a sealing device and a cleaning yet, sooner or later it will be completed.

REFERENCES

- [1] Ty A. Lasky and Bahram Ravani, "Sensor based path Planning and Motion Control for a Robotic System for Roadway Crack Sealing", pp. 609-622, IEEE Trans. On Control Systems Technology, col. 8, No. 4, 2000
- [2] M. Raibert and J. J. Craig, "Hybrid Position/Force Control of Manipulators", *ASME Journal. of Dynamic Systems, Measurements, and Control*, vol. 102, pp. 126-133, 1981
- [3] N. Hogan, "Impedance Control : An Approach to Manipulator, Part i, ii, iii", *ASME Journal of Dynamics Systems, Measurements, and Control*, vol. 3, pp. 1-24, 1985
- [4] H. Seraji, "Adaptive Admittance Control : An Approach to Explicit Force Control in Compliant Motion", *Proc. IEEE Conference on Robotics and Automations*, pp. 2705-2712, 1994
- [5] Seul Jung, T. C. Hsia, "Adaptive Force Tracking Impedance Force Control of Robot for Cutting Process", *IEEE Conference on Robotics and Automations* pp1800-1805, 1999
- [6] R. S. Petty, M. Robinson and J. P. O. Evans, "3D Measurement using Rotating Line-scan Sensors", *Meas. Sci. Technol.* Vol. 9, pp. 339-346, 1998.
- [7] YingLi Tian, SongDe Ma and ManLi- Luo, "3-D Face Image Acquisition and Reconstruction System", *Technology Conference* 1998.
- [8] Witold Czajewski and Andrzej Sluzek, "Development of a Laser Based Vision System for an Underwater Vehicle", *ISIE'99-Bled, Slovenia*, pp. 173-177, 1999.
- [9] Daoshan Yang, Jihong Chen Huicheng Zhou and Shawn Buckley, "Two Practical Ways to Avoid Spurious Reflections from Shiny Surfaces on A 3D Machine Vision Inspection System", *SPEI* Vol. 3652, pp. 30-33, January 1999.
- [10] Stephen Tetlow and John Spours, "Three-dimensional Measurement of Underwater Work Sites using Structured Laser Light", *Meas. Sci. Technol.* Vol. 10, pp. 1162-1167, 1999.
- [11] Witold Czajewski and Andrzej Sluzek, "Development of a Laser Based Vision System for an Underwater Vehicle", *ISIE'99-Bled, Slovenia*, pp. 173-177, 1999.
- [12] Daoshan Yang, Jihong Chen Huicheng Zhou and Shawn Buckley, "Two Practical Ways to Avoid Spurious Reflections from Shiny Surfaces on A 3D Machine Vision Inspection System", *SPEI* Vol. 3652, pp. 30-33, January 1999.
- [13] Stephen Tetlow and John Spours, "Three-dimensional Measurement of Underwater Work Sites using Structured Laser Light", *Meas. Sci. Technol.* Vol. 10, pp. 1162-1167, 1999.